Geophysica (2020), 55(1–2), 3–21

Application of Airborne Gravimetry Data for Litho-Structural and Depth Characterisation of Precambrian Basement Rock (Northwestern Nigeria)

Cyril Chibueze Okpoli and Adedibu S. Akingboye

Department of Earth Sciences, Adekunle Ajasin University, Akungba-Akoko Ondo State, Nigeria

Corresponding author: cyril.okpoli@aaua.edu.ng

(Submitted: November 2, 2018; Accepted: February 25, 2020)

Abstract

This study entails the detailed analyses of high-resolution gravimetry dataset using enhancement techniques for characterising and delineating the locations, edges/boundaries, trends, and depths of litho-structural features around Precambrian basement complex of Igabi region, Northwestern Nigeria with a view of evaluating the structural architectures that harbor mineralization in the study area. The analyzed results of the bouguer anomaly and residual maps of study area showed the distribution of the gravity anomalies and magnitudes of the concealed structures based on the observed low to very high gravity anomalies. Bouguer anomalies around Igabi area ranged between -67.77 to -53.34 mGal reflecting the density variations within bedrock. The upward continued bouguer anomaly maps at distance 500 m, 1 km, 2 km, 3 km, and 4 km revealed the variations of the deep-seated basement rocks, the structures and the concealed anomalous bodies with general regional trends in NW-SE, E-W, and NE-SW directions. The bouguer analytic signal and its superimposed maps further revealed that areas with low amplitude signals may be associated with migmatites, schists, less dense felsic rocks (porphyritic granites) and fractures, and areas of high amplitude signals may be associated with denser biotite granitic and gneissic rocks. In addition, the second vertical derivative and tilt derivative maps clearly revealed the density of shallow basement rocks and near circular closures anomalies associated with fractures within the granitic rocks. Spectral analysis suggests depth to gravity sources range between 0.3 km and 0.67 km for shallow, 0.90 km to 0.97 km for intermediate and 1.5 km to 1.86 km for deep sources while Euler sources depths ranged from <1392.3 m to >2059 m. Based on the calculated bouguer anomalies such as variation in rocks densities, different structures and varying trends of litho-structures in with subsurface depth may have suggested intense deformation of the Basement rocks with varying tectonic framework in the study area over time.

Keywords: litho-structures; characterisation; Bouguer anomalies; spectral analysis; Euler deconvolution

1 Introduction

The dwindling crude oil economics in Nigeria offers the need for diversification of the nation's solid mineral base and resources. The economic potential and minable occurrence of amethyst mineralization (violet variety of α-quartz) in Igabi region, necessitated the aerogravity survey to unravel the character of the subsurface geological structures. The presence of amethyst occurs in several geological environments namely pegmatite dykes, epithermal veins, miarole in granitoids, alpine clefts, geodes in basaltic lavas, calcareous rocks, sandstone and quartzite and agatized tree in Arizona, USA (*Gilg et al.,* 2002; *Solomon*, 2010).

The airborne gravimetry dataset was carried out on Sheet 124, which lies within the Basement Complex of Northwestern Nigeria. The gravity survey is a non-destructive geophysical method that measures difference in the earth's gravitational field at definite locations. Gravity surveys could be carried out at the earth's surface known as "ground gravity survey", or in the air, which is known as "aero-gravity survey". Gravity surveys is used for direct exploration of basement topography and sedimentary basin alongside its structural architecture. In geosciences, it has varied applications, which include engineering exploration, regional and large scales study of geological structures, where measurements of earth's gravitational field are used to map subsurface variations in density (*Mandal et al.,* 2013, 2015; *Biswas et al.,* 2014a, b; *Biswas and Sharma*, 2015, 2016;), *etc*. Gravity interpretation have an objective of recognizing the geological features of the subsurface structures and lithologies from the anomaly maps through innumerable characteristics such as amplitude, shape, sharpness, and frequency of the gravity anomalies, the locations and the structures that produce these gravity characters (*Hesham and Hesham*, 2016).

Aku (2014) applied 2D spectral analysis and second vertical derivative to bouguer data for delineation of lithological boundaries at Gusau area of Nigeria. *Ekpa et al.* (2018) and *Ofoha et al.* (2018) investigated the Niger Delta basin of Nigeria through the interpretation of aero-gravity data to determine the thickness of the sediments, establish the basement topography, density contrasts and structural evaluation which will give information about variations of geological lithologies and structures.

Various gravity enhancement techniques like – Fast Fourier filtering as well as 2D power spectra, Euler deconvolution and analytical signal – offers estimates of the geologic subsurface lithologies and the depth based on the density contrast of the rocks. Fast Fourier transformation of gravity dataset are classified into wavelengths and wavenumber to enhance and suppress the geologic character of interest. The work is aimed at interpreting preliminary high-resolution gravity data through different enhancement techniques to delineate the subsurface lithologies, structures and estimate the depth to top of gravity sources based on the density contrast of the rocks in study area.

2 Geologic setting of the study area

The investigated area lies between longitude 7^{o} 30' and 8 E and latitude 10^{o} 30' and 11N within the Precambrian Basement Complex of Northwestern Nigeria. The area is about 30 kilometers southwest of Kaduna, which extended to about 253.57 km^2 (Figs. 1a and b). The Precambrian rocks of Nigeria may be grouped into three principal subdivisions, which include Migmatite–Gneiss Complex (MGC), Schist Belt (Metasedimentary and Metavolcanic rocks), Older Granites (Pan-African granitoids), Undeformed Acid and Basic Dykes (*Solomon*, 2010). The study area lies in the northwestern part of Nigeria which was affected by two successive phases of intense deformation that resulted to tight isoclinal ENE to WSW and NS axes. These two progressive metamorphism accompanied by deformation, were later separated and followed by static metamorphic phases. These areas are considered to be Upper Proterozoic Supracrustal rocks which have been in folded into the Migmatite-Gneiss-Quartzite complex.

The Basement Complex rocks in the area are grouped into two, namely Migmatite-Gneiss Complex and the Older granites (Pan-African granitoids). The Migmatite-Gneiss Complex is Neo-Proterozoic to Meso-Archean (542Ma-3200Ma) in age and composed of migmatites and gneisses. It is the most extensive rock type in the area. The Older granites (Pan-African granitoids) are Pan-African (600 ± 200Ma) in age and consist mainly of granites, diorites and dolerites. Both the migmatites and gneisses were deformed and intruded by the Pan-African granitoids during the 600 ± 150 Ma Pan-African episodes. The lineaments/faults associated with these Precambrian Basement Complex rocks usually show NE-SW and NW-SE trends (Fig. 1b).

The occurrence of uranium ores is found in the Older granite and mafic schist Igabi, Kajuru, Kalatu and Kachia in Kaduna state as well as Naraguta and Maijuju sheet in Plateau state and all associated Ririwai ring complex in Northcentral Nigeria (*Arisekola and Ayenipa*, 2013). The region is also made up of highly fractured and poorly exposed weathered granitic gneiss and sheared gneiss. The granitic gneiss belongs to the Pan-African Migmatite - Gneiss Complex. It also forms the predominant rock unit as observed in the field. Minor lithological units are minor quartz veins and a prominent vein in which amethyst mineralization occurs and aplite dykes. The structural feature of the study area comprises joints, faults and foliations (*Solomon*, 2010).

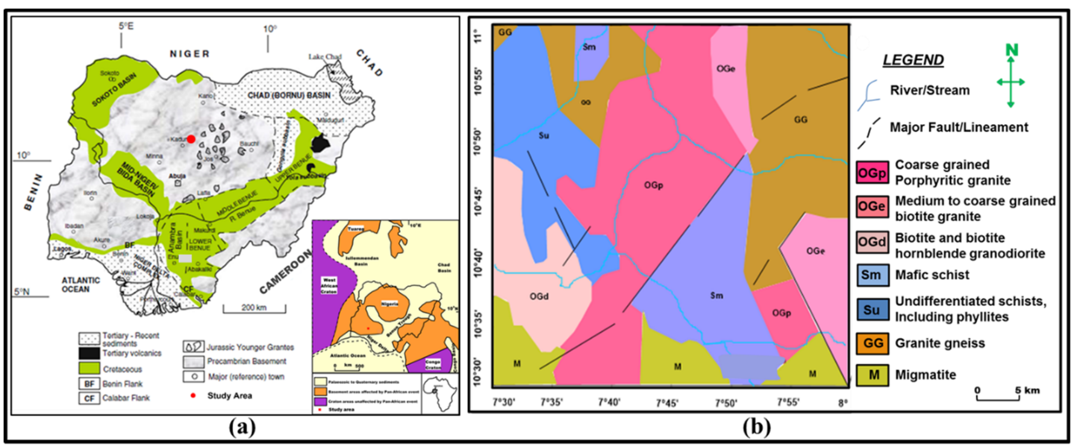

Fig. 1. (a) Regional geological setting of Nigeria showing the study area (modified after *Ajibade et al.*, 1987; *Obaje*, 2009). (b) Geological map of the study area (digitized from *NGSA*, 2009).

3 *Review of previous work*

The earliest study of the Nigeria Basement Complex was carried out by Falconer (1911) during which he identified and distinguished between the Younger and Older Granites. *McCurry and Ajibade* (1987) also classified the younger metasediment as those extensively developed in the North Western part of Nigeria forming N-S trending belt.

Hesham et al., (2016) worked on the reconnaissance study of the eastern area of Quattara Depression using the Bouguer and aeromagnetic data. Several transformation techniques and filtering processes were accomplished on the data. At first, the total magnetic intensity aeromagnetic map was processed through the application of reduction to magnetic north pole techniques. The Fast Fourier Transform was carried out on the gravity and the RTP magnetic data for establishing and defining the residual shallow sources. The high pass filtering was used to enhance the anomaly wavelength associated with shallow sources. The processing techniques were the polynomial surface fitting enhancement, Butterworth high-pass filtering, Euler deconvolution and forward modeling. The result reflected the occurrence of the various types of structures and their component in the study area. The main tectonic deformations of the study area are following NNW – SSW, NE – SW, NW – SE and E – W trends.

Lawal and Osazuwa, (2004) applied the reduction-to-the-pole technique to the aeromagnetic data of the Zaria, Shika, Igabi and Kaduna area, in the north western part of Nigeria. The aeromagnetic data used for the work was obtained by digitizing six aeromagnetic maps which covered the area. The aeromagnetic dataset used in the survey were obtained from the Nigerian Geological Survey Agency which include Sheets 101, 102, 103, 123, 124 and 125. Oasis Montaj and Surfer 8 software were deployed to perform and interpret the general three dimensional case. After reducing the data to the pole, and comparing it to the total field, it was seen that the technique eliminates the dipolar nature of the anomalies. The presence of positive anomalies observed from the result for most parts of the area validates the assumptions of induced magnetization within the area. The magnetization map computed using the reduced to the pole field reveal some unexposed granitic intrusions within the area covered.

Raimi et al., (2014) studied in details the structural interpretation of the Aeromagnetic Field over a Region in the Nigerian Younger Granite Province. As revealed by the geological map, the study area is largely covered by basement rocks while the rest is covered by Ring Complexes. The basement rocks consist of two groups; the ancient metasediments that are considered to be older than 2000 m.y and the group that mainly consist of migmatite, granite-gneisses and Older Granites that is believed to have resulted from remobilization during the Pan-African orogeny. This basement has been subjected to different episodes of folding and faulting. The dominant foliation is roughly north-south with variations between NW-SE and NE-SW. Fractures and shear zones also characterize the basement. They consist of E-W trending fractures, which are perhaps the oldest fractures and almost obliterated. Others are N-S fractures that resulted from brittle deformation and twin conjugate sets of NE/SW and NW/SE and the NNE/SSW and NNW/SSE sets, produced by transcurrent movements.

George et al., (2015) qualitatively and quantitatively interpreted the Aerogravity and magnetic data over the south western part of the Volta River Basin of Ghana. Field data correction and reductions were applied to the acquired data to enhance the data for better interpretations. Low-to-moderate-to-high gravity and magnetic anomalies were obtained in the Complete Bouguer Anomaly (CBA) and Total Magnetic Intensity (TMI) reduction to pole with many of these anomalies trending NE-SW, in which the Birimian Metasediments and Metavolcanics can be said to be part of the causative structures of these anomalies with cross-cutting to produce NW-SE faults. From the Euler deconvolution, the intrusive granitic bodies of the study area have a mean depth location of 1.7 km, while the isolated anomaly is located at a depth of 1.4 km. The NE-SW trending anomalies show the regional trend of the causative bodies, the basement rocks and the basinal intrusive bodies.

Ayodeji and Odumade, (2015) worked on geological and structural interpretation of Ado-Ekiti southwest and its adjoining areas using aeromagnetic data. The dataset was collected, filtered, inverted, and enhanced using appropriate software packages and subsequently employed to generate a model of the subsurface basement topography. The data processing steps involved were Butterworth filtering, reduction to the equator, analytic signal, upward continuation, tilt angle derivative, average power spectrum, Euler deconvolution, and window Euler solution. The analytical signal derivative map accentuates the variation in the magnetization of the magnetic sources in the study area and highlights discontinuities and anomaly texture. Three major magnetic zones i.e. high magnetic anomalous zone were defined as (BM), intermediate magnetic anomalous zone (BQ) and low magnetic anomalous zone (BG). Comparative study of the original geological map and proposed geologic map of study area and its adjoining areas were done. It showed that structural lineaments are nearly evenly spread across the different rock types and are relative to the positions of the volcanic intrusions and quartz veins spotted on the migmatite rock on the original geological map indicating that both maps correspond.

4 Materials and methods of study

The purpose of gravity study is to locate and describe subsurface structures from the gravity effects caused by their anomalous densities (*Lowrie*, 2007; *Telford et al.*, 1990). The variations in acceleration due to earth's gravity are caused by variations in subsurface geology. The aero-gravity data was acquired from Nigerian Geological Survey Agency (NGSA) in Geosoft file format. The aerogravity were acquired in 2013 using specially designed transportable spring-mass Micro-g Lacoste Turnkey Airborne Gravity System (TAGS) mounted on gyrostabilized platforms. The survey instrument is the TAGS' AIR III gravimeter, a beam- type, zero- length spring gravity sensor on a gyrostabilized platform Micro-g lacoste. This modern gravimeter measures to 0.01 mGal resolution, accuracy of 1.0 milliGal or better, static repeatability of 0.05 milliGal and dynamic repeatability: 50,000 milliGal horizontal acceleration =0.25milliGal, 100,000 horizontal acceleration = 0.50 milliGal and 100,000 milliGal vertical acceleration of 0.25 milliGal. The surveys were conducted by Fugro Airborne Surveys, Canada, under the supervision of Nigeria Geological Survey Agency (NGSA).

The agency applied some sorts of reductions/corrections like latitude, elevation, terrain/topography, bouguer, free air and Eotvos. High resolution bouguer gravity dataset was measured at a terrain clearance of about 100 m, flight line direction of NE-SW, flight line spacing of 500 m and tie line spacing of 4000 m as well as aircrafts covering a total of 235,000 line kilometers. The modelling software that were used for the processing, analysis and interpretation of the bouguer datasets include Geosoft® Oasis Montaj™ software version 6.4.2 H. J, and Surfer ™ Version 12.

The resolution of the bouguer grid has a recording interval of 0.1 secs and a grid mesh of 50 m which were applied to the world Geodetic System of 1984 (WGS84). Structures like dike-like intrusives, faults, folds, joints were interpreted from the dataset. The acquired bouguer anomaly gridded dataset was re-projected from zone 32N (UTM) to zone 31N (UTM) in order to align the gridded data with their actual coordinates. Thereafter, various forms of data derivatives and enhancement techniques were applied to the bouguer anomaly dataset. The data derivatives and enhancement techniques include residual field, Second Vertical Derivative (SVD), Analytic Signal (AS), Tilt-angle derivative, and upward continuation. We make use of the upward continuation enhancement technique to smoothen out shorter wavelength anomalies after determination of the gravity field at an elevation higher than that at which the gravity field is measured (*Hakim et al.,* 2006). We utilized the second vertical derivative in gravity interpretation to enhance localized small and weak near-surface features; which involves the improvement of the resolving power of the gravity map that has long been established (*Baranov*, 1975; *Gupta and Ramani*, 1982). We quantitatively interpreted the depths estimates and dimensions of sources of anomalies. The quantitative techniques adopted in this study include: spectral analysis using Radially Averaged Power Spectrum (RAPS) and 3-dimensional Euler deconvolution.

5 Discussion of Results

The analyzed re-projected bouguer anomaly (Fig. 2) ranged from -67.77 to -53.34 mGal denoting variations in density properties of rocks. The negative bouguer anomaly amplitude result is owed to the mountainous regions, where the survey was carried out; thereby reducing out the attraction of the mountainous mass (*Karner and Watts*, 1983). While very high positive gravity anomaly (-53.34 mGal) marked A seen as a circular closure in the southwestern part of the area indicates the presence of subsurface denser rocks. The northeastern and southeastern parts of the area marked B show areas with very low gravity anomalies (< -66 mGal), which may be attributed to presence of less dense and deformed rocks present in the study area. The central part of the area is characterized by fairly low to moderately high gravity anomalies (-66 mGal to -64.5 mGal) marked C as sub-rounded shapes to an approximately straight linear trends of NW-SE and NE-SW directions, which may be suggested as the fractured zones, edges and contacts of different rocks in the area. Generally, most of the anomalies present in the area are trending NW-SE direction.

The regional bouguer gravity field was produced by upward continuing the bouguer anomaly data up to 4 km. The regional gravity field was then subtracted from the observed bouguer anomaly (Fig. 2) to produce the residual bouguer gravity anomaly (Fig. 3). The later reflects the distribution of lateral density variations within the crust and highlights concealed lithologies.

Figure 3 displays maximum anomaly value of 1.60 mGal at the northern and southwestern parts and minimum anomaly value of less than −1.33 mGal at the western, northeastern, pocket at eastern section and central section of the study area extending to northwestern section of the study area. The strong high gravity anomalies marked A at the southwestern, northeastern and the eastern part of the area may suggest the presence of subsurface shallower or near surface uplifted and denser basement rocks. Low to moderate gravity anomalies revealed at the northwestern and southwestern end, as well as the central to the northwestern end of the study area may possibly be less dense rocks i.e. rocks of lower density, which may have been affected by intense metamorphism that produced the observed lineaments/faults in the area. The anomalies in the study area occur in different shapes and polarities, as well as showing a general trends and patterns in WNW-ESE, NW-SE, and NE-SW directions.

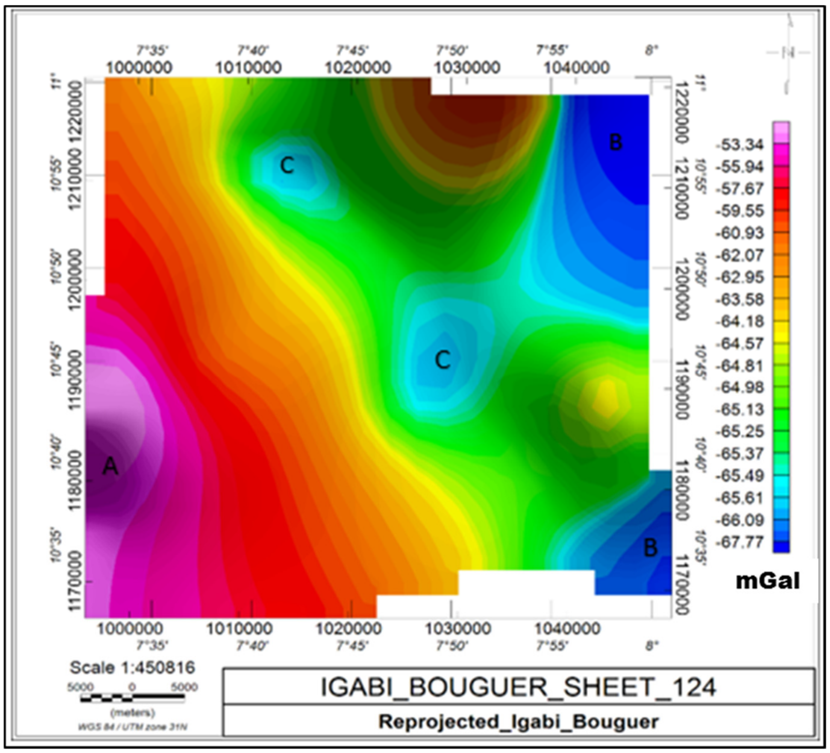

Fig. 2. Bouguer anomaly map of the study area. *Points A and B indicate area of very high and very low gravity anomalies respectively while points annotated as C are areas with relatively low gravity anomalies*.

The upward continuation enhancement method shows clearly the attenuation/reduction of short-wavelength anomalies with respect to the increase in observation to source distance (*Ganiyu et al.,* 2013). The upward continuation serves to smooth out near-surface effects (shorter wavelength anomalies) after calculating the gravity field at an elevation higher than that at which the gravity field is determined (*Hakim et al.,* 2006). Upward continuation filter was used in suppressing the effect of shallow anomalies, in order to acquire information on deeper anomalies. Figures 4a-e shows the maps of the upward continued bouguer anomaly data to 500 m, 1 km, 2 km, and 3 km and 4 km respectively. The most important effects of this filter on the data are basically to infer the effects of depth of continuation on gravity sources which are associated with the basement rocks and geological structures, as well as to reveal the regional basement anomaly trends.

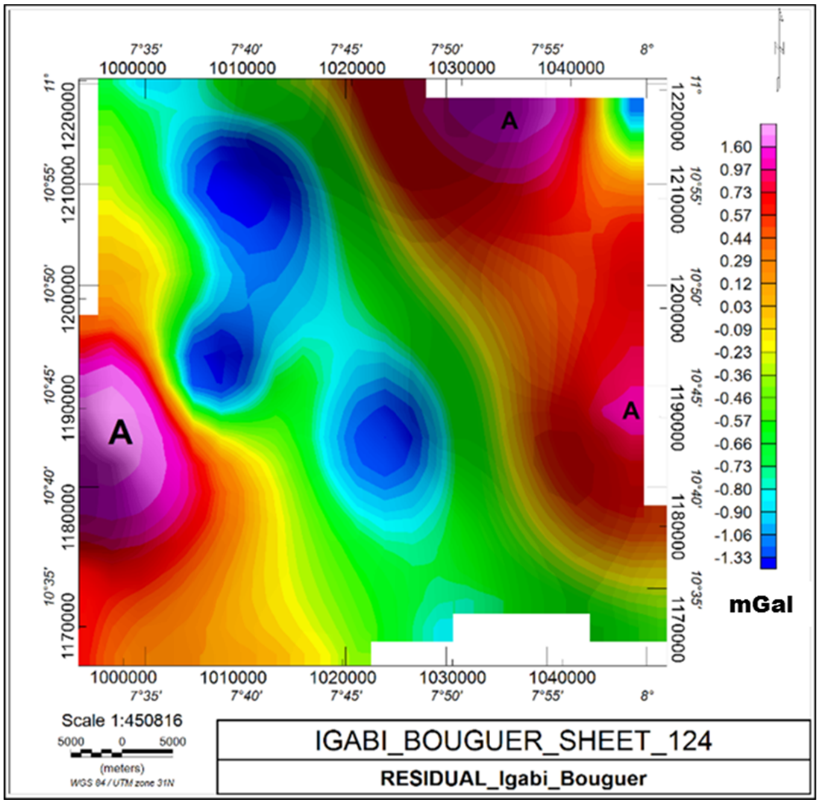

Fig 3. Residual bouguer anomaly map of the study area. **Point A maps areas with denser crustal rocks within the study area.*

Generally, all the upward continuation maps reflect varying gravity anomalies with respect to depth of upward continuation. High to very high gravity anomalies (>-64 mGal) occupy a portion of about half of the study area towards the western parts with an approximate trend in NW-SE direction while very low to intermediate gravity anomalies (<-64 mGal) occupy the other half. High gravity anomaly is also revealed at the northern end of the study area (Figs. 4a, b, and c) as a circular closure, but the anomaly reduces with upward continuation depth above 2 km and disappears with depth of continuation above 3 km (Figs. 4d and e). Areas occupied by high to very high gravity anomalies suggest subsurface denser rocks. On the other hand, intermediate gravity anomaly at the central part with similar trend of NW-SE, and very low to low anomalies with trend of approximately NE-SW may be regarded as lineaments/faults that host viable economic minerals in the areas, such as Amethyst in granite gneiss (*Arisekola and Ajenipa*, 2013). The width of the two circular very low gravity anomaly closures increases with depth of continuations; the two closures finally joined with changed in trending direction to NW-SE at depth of upward continuation from 3 km and above (Figs. 4d and e). These variations in widths and trends suggested that the earlier delineated lineaments/faults with NE-SW trends (Figs. 4a, b, and c) have shallow to intermediate depth and may probably have formed at a later time while those in NW-SE are at deeper depth and may have been formed contemporaneous with the rocks in the area.

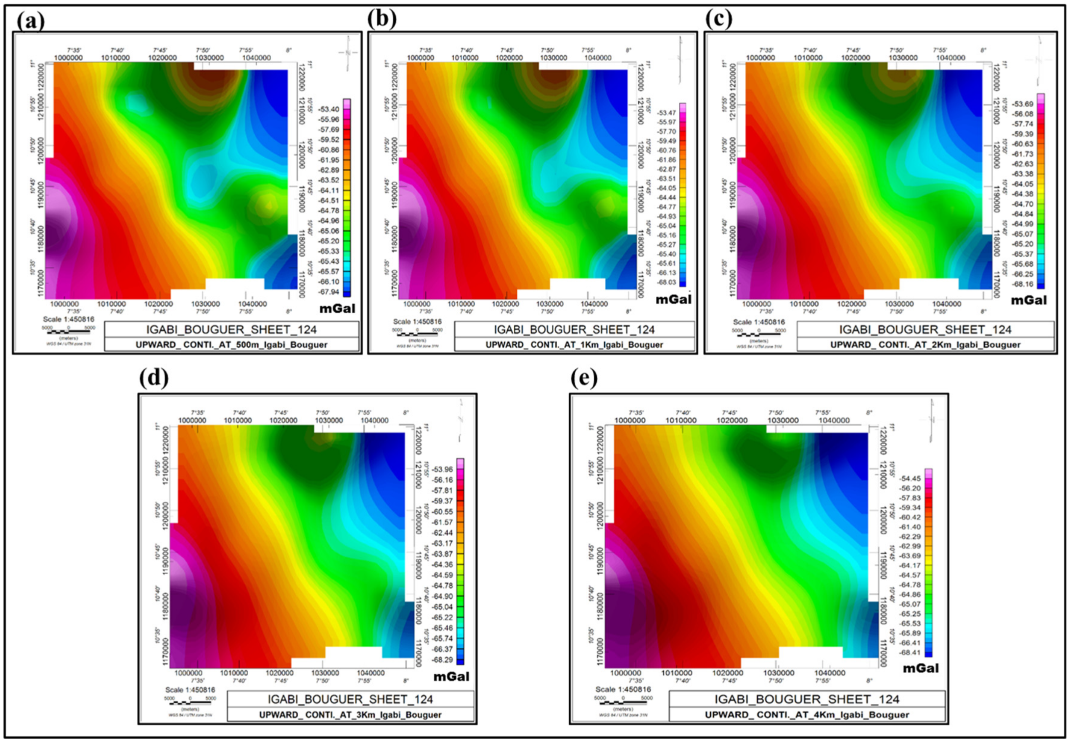

Fig. 4. Upward continuation of Igabi bouguer anomaly to 500m (a), 1km (b), 2km (c), 3km (d) and, 4 km (e).

Figures 5a and b show the bouguer anomaly analytic signal map and the superimposed map of the analytic signal map on the geological map of the study area respectively. The analytic signal method, also known as the total gradient method, produces a particular type of calculated gravity anomaly enhancement map used for defining the edges (boundaries) of geologically anomalous density distributions (*Hakim et al.,* 2006). The use of analytic signal amplitude (*Nabighian*, 1972; 1974) poses attractive features for any sort of potential field prospecting. Its advantageous geophysical property is that it peaks exactly over the edge of the buried dipping contact that causes the magnetic anomaly (*Nabighian*, 1972). The analytic signal filter produces a particular type of calculated magnetic anomaly enhanced map used in defining edges (boundaries) of geological anomalous magnetization distribution present in maps. It can also be used to determine depth of the anomaly sources. The bouguer analytic signal map (Fig. 5a) shows high amplitude signal values that ranged above 0.006 mGal/m at the western and northeastern parts denoted as P4 and P5 respectively. These areas of high analytic signals may probably be due to high density contrasts generated by denser and shallower biotite granitic and gneissic rocks (Fig. 5b). Points P1 and P2 are points of very low amplitude signal (0.0001 – 0.002) mGal/m with a NW-SE trend, these zones are suggested as highly fractured migmatites, schistose and less dense felsic rocks (porphyritic granites). The highlighted arrows on the map mark some of the edges/boundaries of rocks and also show the zones of weaknesses that are majorly lineaments/faults with approximate trends in NW-SE and NE-SW (parts with oblong curves along the low amplitude signal axis) directions. The superimposed map (Fig. 5b) further confirms the litho-structural relationships that exist in the study area based on varying density contrasts revealed by the rocks. Figure 5b also shows that most of the delineated and mapped subsurface lineaments/faults by the analytic signal enhancement technique correspond with the directions of the major surface fractures on the geological map.

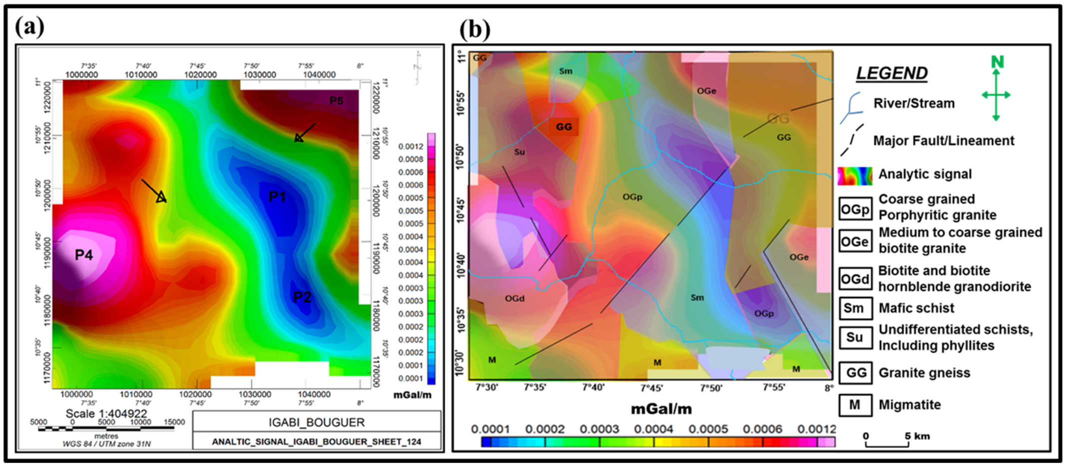

Fig. 5. (a) Bouguer Anomaly Analytic Signal Map. (b) Superimposed map of the bouguer anomaly analytic signal map on the geological map of the study area to show the relationship between Analytic Signal of the subsurface rocks and surface rocks in the Study Area. *P1, P2, are points of very low amplitude signals while P4, P5 are points of high signal values.*

The second vertical derivative (2VD) technique is one of several methods of removing the regional trend. Some gravity anomalies may be distinct on examination of the bouguer map, but weak anomalies arising from shallower sources of limited depth and lateral extents may be obscured by the presence of stronger gravity effects associated with deeper features of larger dimensions (*Aku*, 2014). The second vertical derivative filter sharpens the edges of anomalies which aid in locating their positions. The application of the second vertical derivative in gravity interpretation to enhance localized small and weak near-surface features (i.e. improving the resolving power of the gravity map) has long been established (*Baranov*, 1975; *Gupta and Ramani*, 1982).

The second vertical derivative (2VD) bouguer anomaly map (Fig. 6) reveals that some of the anomalies have been accentuated and re-positioned when compared to the bouguer anomaly map (Fig. 2), though still evinced relatively similar features compared with the residual bouguer map (Fig. 3). High gravity anomalies >0.0001 mGal/m occupy parts of the northern, eastern and the southwestern (marked as A) sections; indicating that the rock types present in the area are denser than other rock types in the area. Point L with intermediate gravity anomaly may probably be an alteration zone of shallower depth. Point B and C show areas of low to fairly low gravity anomaly which may be associated with fractured rocks in the area. This map reveals that the general trends of the shallower anomalous bodies are mainly NW-SE, NE-SW, and E-W (minor) directions.

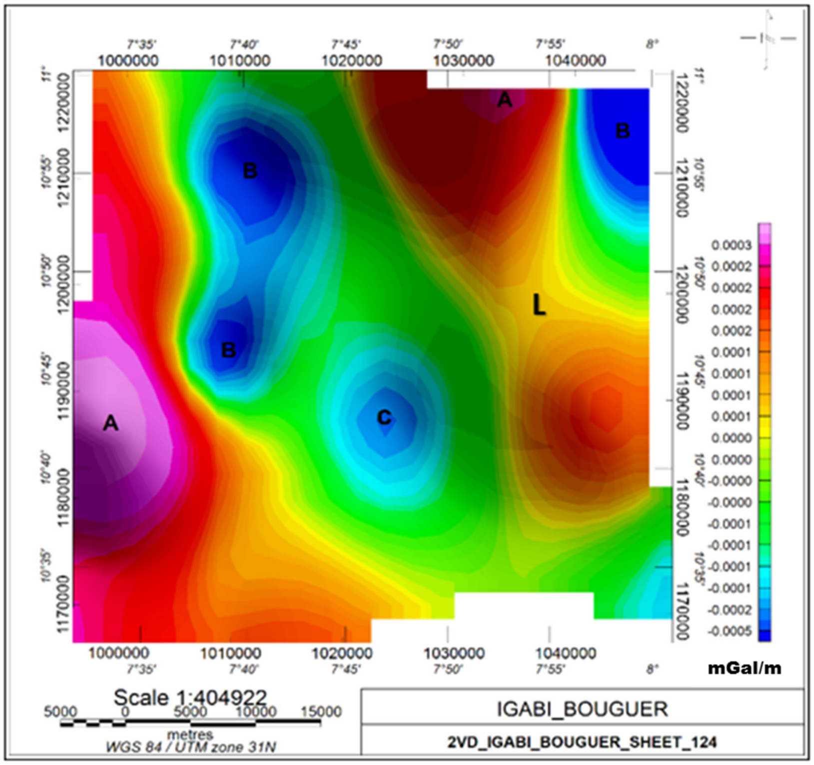

Fig. 6. Second vertical derivative (2VD) bouguer anomaly map. Regions marked A and L indicate areas with very high and intermediate gravity anomalies respectively while points B and C indicate areas with very low to low gravity anomalies respectively.

The Tilt Derivative (TDR) filter attempts to place an anomaly directly over its source (*Okpoli and Oladunjoye*, 2017). TDR assists in estimating contact locations of bodies at depth (*Ndousa-Mbarga et al.,* 2012; *Oyeniyi et al.,* 2016), and identifying areas of anomaly structures that are least affected by interference where repeated depth estimates are most likely to be reliable (*Salem et al.,* 2007).

The bouguer TDR (Fig. 7) maps the anomalous conditions of the subsurface and is indicated by successive closed contours represented by high and low frequency gravity anomalies on the map. The region enclosed by the 0º and distance between +45° and -45° (±1.5 radians) contours indicates the approximate location of the source edges and shallow basement rocks respectively. The horizontal distance from the 45° to the 0° position is equivalent to the depth to top of the contact, or half distances between +45° and -45° (*Al-Badani and Al-Wathaf*, 2017). The circular to oblong closures anomalies observed around the central region of the western part of the bouguer map may be associated with granitic bodies in the area. Points denoted A is classified as area of very high gravity anomaly probably due to denser and shallow basement rocks. Points B mark the edges of the zone of weaknesses in the area; the deformed basement rocks confined the edges and trends of the pronounced lineaments/faults mainly in NW-SE direction as seen at the central half of the map.

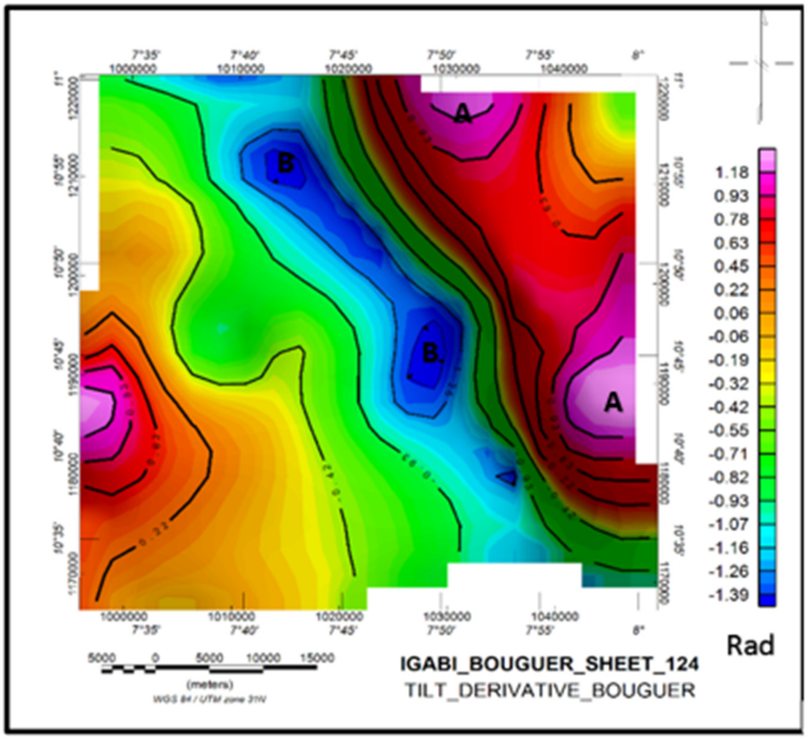

Fig. 7. Contoured colour shaded tilt derivative bouguer map of the study area. Points A and B are points of high and low frequency gravity closures respectively.

Figure 8 shows the Radially Averaged Power Spectrum (RAPS) or spectral analysis of the bouguer anomaly data. Power Spectrum is a 2-D function of the energy and wave number and is generally used to identify the average depth of source assemblages (*Spector and Grant*, 1970). Spectral analytical tool is a well-established tool for estimating the depths of magnetized bodies (*Bhattacharyya*, 1966; *Mishra and Naidu*, 1974; *Blakely*, 1996; *Emberga and Timothy*, 2014). Several authors, such as *Spector and Grant* (1970); *Bhattacharya* (1994); *Garcia and Ness* (1994); *Tatiana and Angelo* (1998), explained the 2-dimensional radial spectrum technique. The bouguer anomaly map was divided into two spectral blocks to calculate their radially averaged spectrum (Figs. 8a and b). Three depth sources which include shallower, intermediate and deeper sources were delineated on the 2-D spectrum of respective spectral blocks based on wavelengths of density anomalous sources. The deeper source (red line), the intermediate source (yellow line) and the shallower source (blue line).

The coordinates and various depths to top of density sources for respective quadrants are shown in Table 1. The shallower, intermediate, and deeper depths are 0.3 km, 0.9 km and 1.9 km and 0.2 km, 1.00 km, and 1.9 km for spectral block 1and 2 respectively. These estimated depths are only to the top of anomalous density sources in the area.

Table 1. Depth estimates to top of gravity sources derived from spectral analyses.

Spectral block	Easting (mE)		Northing (mN)		Depth (km)		
	X_{min}	X_{max}	Y_{min}	Y_{max}	Shallower	Intermediate	Deeper
1	992293	1022518	1190546	1219530	0.30	0.90	1.90
2	1019247	1047104	1189530	1219869	0.20	1.00	1.90

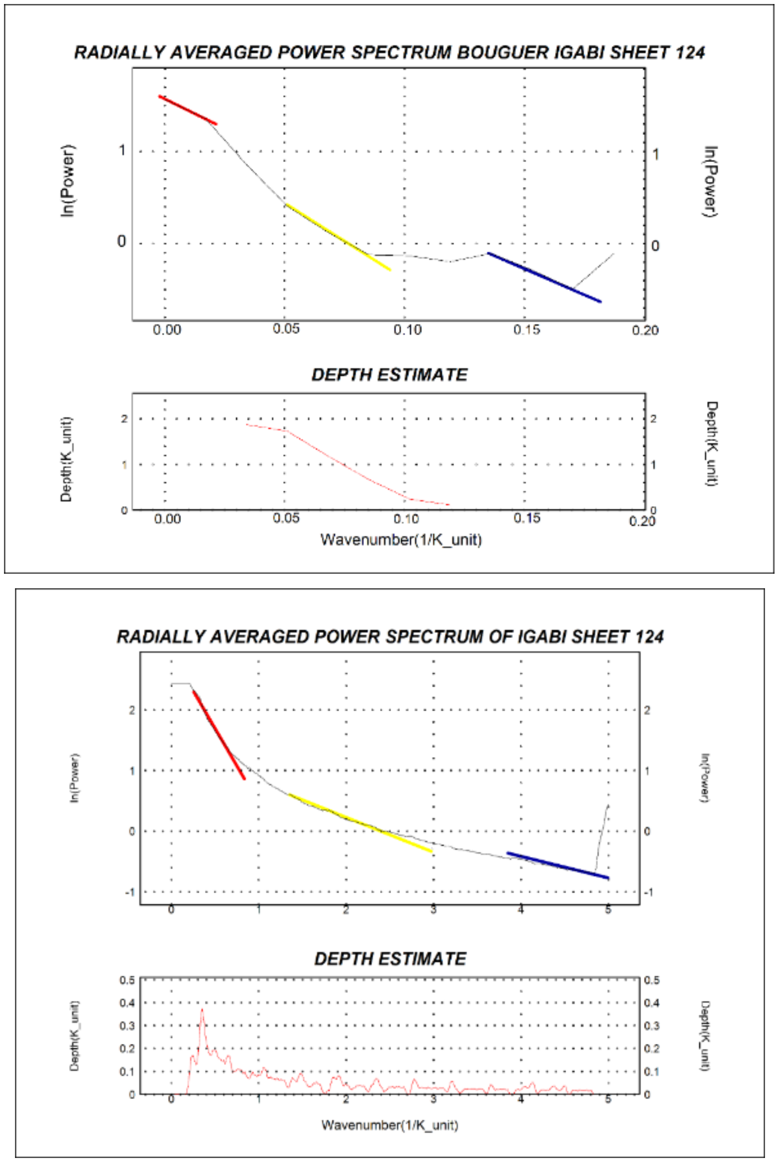

Fig. 8. Spectral analysis of the Igabi bouguer anomaly data.

Keating (1995) applied 3–dimensional Euler deconvolution technique to aerogravity and aeromagnetic dataset, while *Klingele et al.,* 1991 interpreted for gravity vertical gradient and Zhang *et al.,* 2000 utilized the tensor gravity gradient. 3-dimensional Euler deconvolution has further been extended and generalized to cope with a wider range of source types (*Mushayandebvu et al.,* 2001; *Ravat et al.,* 2002; *Stavrev and Reid,* 2007, 2010).

Euler deconvolution structural index (S.I) of different source types, namely S.I 0.0, S.I 1.0, and S.I 2.0 were applied to bouguer anomaly data used for this study. S.I 0.0 is used for delineating line cylinder, thin sheet edge, thin sill and dyke; S.I 1.0 for delineating line cylinder and thin line belt, and S.I 2.0 delineates point and sphere (*Reid et al.,* 2013*)*. Euler deconvolution technique was not only used for delineating subsurface structures but also for determining the average depth of the gravity sources (*Sultan et al.,* 2017).

The structural solutions result (Figs. 9a, b, and c) are scanty, but still reveal the different structural index models: locations, edges and trends of different subsurface structures, as well as depths to the anomalous sources. S.I 0.0 solution result (Fig. 9a), reveals some of the trends and edges (indicated by arrows) of the thin sheet and thin dykes/sills with approximate trend of NW-SE and indication of tectono-metamorphic

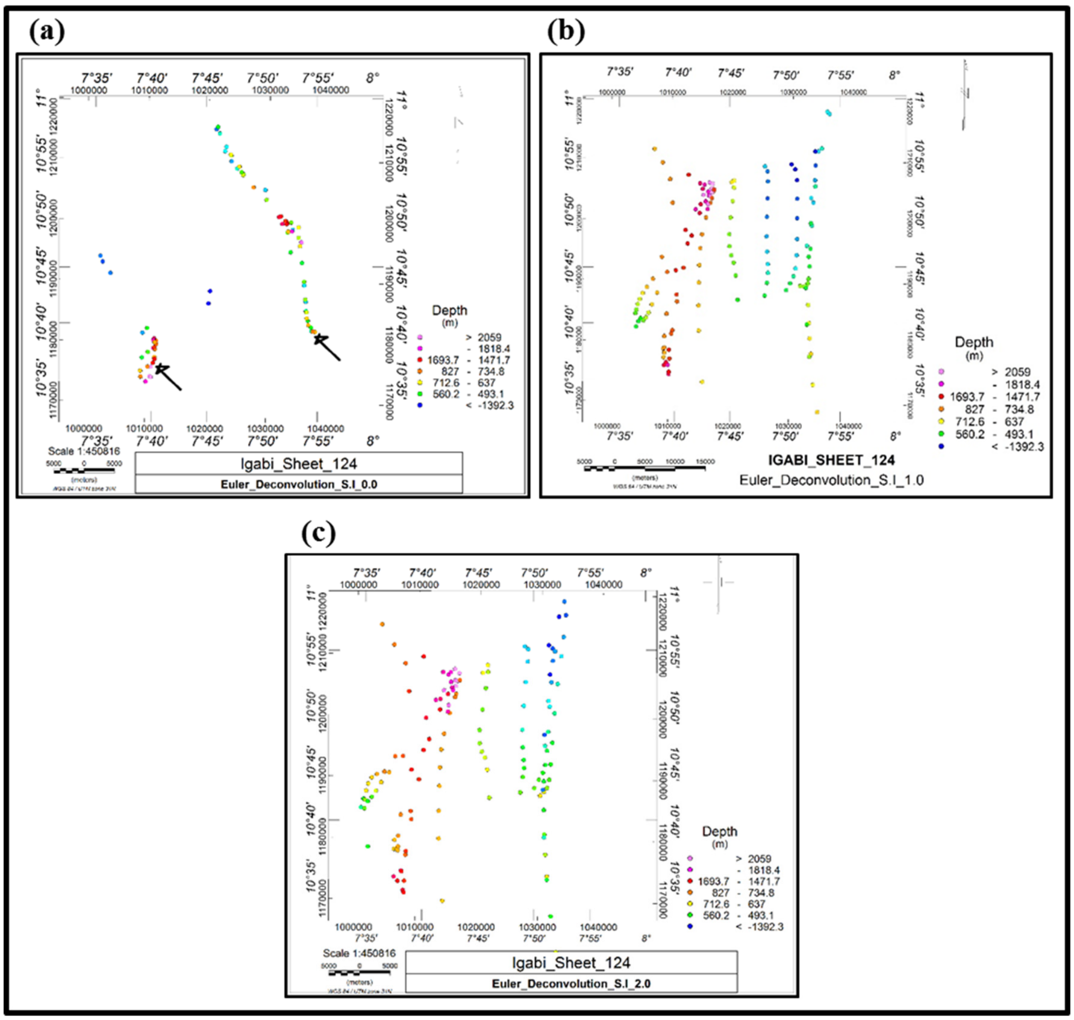

Fig. 9. Euler deconvolution solutions of the bouguer anomaly data for S.I 0.0 (a), S.I 1.0 (b), and S.I 2.0 (c).

phases of Pan African orogeny. S.I 1.0 solution result (Fig. 9b) clearly reveals the line cylinders, and S.I 2.0 solution result (Fig. 9c) was able to show the point and spherical structures in the study area. All the Euler deconvolution structural indices solutions showed that the lithological structures in the study area are mainly concentrated at central part while other parts like the western, northern and southern sections of this area have fewer structural features. These results further confirm that the central part and small parts of the western, northern and southern sections of the study area are characterized by highly deformed and fractured schistose rocks while the granitic rocks of these area are probably intrusive dykes. The obtained Euler anomalies depths ranged from <1392.3 m to >2059 m over the mining zones suggesting that the mineralization is structurally controlled.

The structural indices of pipes, ring-like and sphere models when applied were readily consistent with the delineated areas as observed from the contact/dyke models. The surplus of a definite solution for a structural index of 2 and 3, diagnostic of pipe, sphere or ring-like massive anomalous body, might suggest that the ore bodies are concentrated as observed from the presence of large scale mining in the study area (Fig. 9).

6 Conclusion

In this study, high-resolution bouguer data analyses and enhancement techniques were carried out to reveal the locations, edges/boundaries, trends, and depths of litho-structures around the study area (Sheet 124 NE), Northwestern Nigeria. These features were revealed through different range of gravity anomaly values that suggest different rock types of varying density contrasts and deformations.

The analyzed results of the bouguer anomaly and residual maps of study area show the distribution of the gravity anomalies and magnitudes of the concealed shear and weak zones being characterised by low to very high gravity anomalies. The upward continued bouguer anomaly maps at distance 500 m, 1 km, 2 km, 3 km, and 4 km reveal the variations of the deep-seated basement rocks, the structures and the concealed anomalous bodies with depth; the maps also show that the regional trends of the mapped lithologies and lineaments/faults in the area are generally in NW-SE, E-W, and NE-SW directions. Furthermore, the bouguer analytic signal and its superimposed maps reveal areas with low amplitude signals as regions with probably migmatites, schistose, less dense felsic rocks (porphyritic granites) and fractures, and areas of high amplitude signals which may have been characterized by denser biotite granitic and gneissic rocks; the maps also show some of the lineaments/faults of the area to be trending in NW-SE and NE-SW directions. In addition, second vertical derivative (2VD) bouguer anomaly map reveals that parts of the northern, eastern and the southwestern sections of the study area are characterized by denser basement rock than other parts, especially the central part of the study area.

For litho-structural and depth characterization, TDR, RAPS and Euler deconvolution were employed. TDR map showed circular to oblong closures anomalies observed around the central region which may be associated with fractures within the granitic bodies in the area. It also maps out the edges of the basement rocks and the intra-basement lineaments/faults with trend mainly in NW-SE direction. The spectral analysis of the RAPS results suggests depth to top of gravity sources between are 0.3 km, 0.9 km; 1.9 km, 0.2 km and 1.00 km, 1.9 km for shallow, intermediate and deep sources. On the other hand, the Euler solutions mapped different subsurface structural features that include thin sheets and thin dykes/sills (with trend of NW-SE), line cylinder and sphere, as well as depth of Basement rocks that ranged between less than 1392.3 m to depth over 2054 m. The amethyst mineralization in the study area are believed to be hosted in shallow zones and structurally controlled in NW-SE direction.

Based on the measured bouguer anomalies such as variation in rocks densities, different structures and varying trends of litho-structures with subsurface depth may have suggested intense deformation of the Basement rocks with varying tectonic framework in the study area over time.

Acknowledgements

We are grateful to Nigerian Geological Survey Agency (NGSA) for providing the Aerogravity dataset used in this study.

References

Ajibade, A.C, M. Woakes and M.A. Rahaman, 1987. Proterozoic Crustal Development in the Pan-African Regime of Nigeria: Amer. Geophysics. Union, 259-271.

Aku, M.O., 2014. Application of second vertical derivative analytical method to bouguer data for the purpose of delineation of lithological boundaries. *Science World Journal,* Vol. **9**, No. 3, pp. 27–32.

Al-Badani, M.A. and Y.M. Al-Wathaf, 2017. Using the aeromagnetic data for mapping the basement depth and contact locations, at southern part of Tihamah region, western Yemen, Egypt. *Egyptian Journal Petroleum.*, DOI:10.1016/j.ejpe.2017.07.015.

Arisekola T.M. and R.A. Ajenipa, 2013. Geophysical data results preliminary application to uranium and thorium exploration. *IAEA-CYTED-UNECE* workshop on UNFC-2009 at Santiago, Chile 9–12, July, 12.

Ayodeji, J. and D. Odumade, 2015. Geological and Structural Interpretation of Ado-Ekiti Southwest and its Adjoining Areas Using Aeromagnetic Data. Adapted from AAPG, SEG and SEPM Joint Technical Conference, Oxnard, California. pp. 1–10.

Bhattacharyya, B.K., 1966. Continuous spectrum of the total magnetic field anomaly due to a rectangle prismatic body. *Geophysics,* Vol. **31**, pp. 97–121.

Baranov, V., 1975: *Potential fields and their transformations in Applied Geophysics*. Exploration Monograph Series, Vol. **65**, pp. 58–69.

Biswas A., A. Mandal, S.P. Sharma and W.K. Mohanty, 2014a. Delineation of subsurface structure using self-potential, gravity and resistivity surveys from South Purulia Shear Zone, India: *Implication to uranium mineralization Interpretation*, Vol. **2**, No. 2, pp. 103–110.

Biswas, A., A. Mandal, S.P. Sharma and W.K. Mohanty, 2014b. Integrating apparent conductance in resistivity sounding to constrain 2D Gravity modeling for subsurface structure associated with uranium mineralization across South Purulia Shear Zone. *Int. J. Geo.* pp. 1–8.

Blakely, R.J., 1996. *Potential Theory in Gravity and Magnetic Applications*. Cambridge University Press, U.K.

Digitized Geological Map of Nigeria 2009. Nigerian Geological Survey Agency (NGSA), Garki, Abuja.

Ekpa, M.M., M.I Okeke, F.N. Ibuot, J.C. Obiora and D.N. Abangwu, 2018. Investigation of gravity anomalies in parts of Niger Delta Region in Nigeria using aerogravity data. *International journal of physical sciences.* Vol. **13**, No. 4, pp. 54–65. DOI:10.5897/IJPS2017.4700.

Falconer, J.D. 1911. The geology and Geography of Northern Nigeria McMillan; London, 295 p.

Garcia, J.G. and G.E. Ness, 1994. Inversion of the power spectrum from magnetic anomalies. *Geophysics,* Vol. **59**, pp. 391–400.

Ganiyu, S.A., B.S. Badmus, M.O. Awoyemi, O.D. Akinyemil and T.O. Oluwaseun, 2013. Upward Continuation and Reduction to Pole Process on Aeromagnetic Data of Ibadan Area, South-Western Nigeria. *Earth Science Research,* Vol. **2**, No. 1, pp. 66–73. DOI:10.5539/esr.v2n1p66.

George, H., M. Agboagye and D.W. David, 2015. Qualitative Interpretation of Aerogravity and Aeromagnetic Survey Data over the South Western Part of the Volta River Basin of Ghana. *International Journal of Scientific & Technology Research*, Vol. **4**, Issue 04, pp. 23–30.

Gilg, H.A., G. Morteani, Y. Kostitsyn, C. Preinfalk, I. Gatter and A.J. Streider, 2002. Genesis of amethyst geodes in basaltic rocks of the Serra Geral Formation (Ametista do Sul, Rio Grande do Sul, Brazil); a fluid inclusion, REE, oxygen, carbon, and Sr isotope study on basalt, quartz, and calcite. *Mineralium Deposita*, **38**, 1009–1025.

Gupta, V.K. and N. Ramani N. 1982. Optimum second vertical derivatives in geologic mapping and mineral exploration. *Geophysics,* Vol. **42**, pp. 1706–1715.

Hakim, S., N. Jun, E. Sachio and A. Essam, 2006. Integrated gradient interpretation techniques for 2D and 3D gravity data interpretation. E*arth Planets Space*, Vol. **58**, 815–821.

Hesham, S.Z. and T.O. Hesham, 2016. Application of high-pass filtering techniques on gravity and magnetic data of the eastern Qattara Depression area, western Desert, Egypt. *Journal of Astronomy and Geophysics,* Vol. **5**, No. 1, pp. 106–123.

Karner, G.D. and A.B. Watts, 1983. Gravity anomalies of the lithosphere at Mountain Ranges. *Journal of Geophysical Research,* Vol. **88**, No. B12, pp. 10.499–10.477.

Klingele, E.E., I. Marson and H.G. Kahle, 1991. Automatic interpretation of gravity gradiometric data in two dimensions: vertical gradient. *Geophysical Prospecting,* Vol. **39**, pp. 407–434.

Lawal, K.M. and I.B. Osazuwa, 2004. Reduction to the pole of the aeromagnetic data of Zaria area, north central Nigeria. *Bollettino di geofisica teorica ed applicata*, Vol. **45**, No. 1–2, pp. 89–95.

Lowrie, W. 2007. *Fundamentals of Geophysics*. Cambridge University Press, London.

Mandal, A., A. Biswas, S. Mittal, W.K. Mohanty, S.P. Sharma, D. Sengupta, J. Sen and A.K. Bhatt, 2013. Geophysical anomalies associated with uranium mineralization from Beldih mine, South Purulia Shear Zone, India. *J. Geol. Soc. Ind.,* Vol. **82**, no. 6, pp. 601–606.

Mandal, A., W.K. Mohanty, S.P. Sharma, A. Biswas, J. Sen and A.K. Bhatt, 2015. Geophysical signatures of uranium mineralization and its subsurface validation at Beldih, Purulia District, West Bengal, India: A case study. *Geophysical Prospecting,* Vol. **63**, pp. 713–726.

Nabighian, M.N., 1972. The analytic signal of two-dimensional magnetic bodies with the polygonal cross-section: its properties and use for automated anomaly interpretation, *Geophysics,* Vol. **3**, No. 37, pp. 507–517.

Nabighian, M.N., 1974. Additional Comments on the Analytic Signal of Two-Dimensional Magnetic Bodies with Polygonal Cross Section, *Geophysics,* Vol. **39**, pp. 507–517.

Ndousa-Mbarga, T., A.N.S. Fenmoue, E. Manguelle-Dicoum and J.D. Fairhead, 2012. Aeromagnetic data interpretation to locate buried faults in south-East Cameroon. *Geophysica,* Vol. **48**, No. 1–2, pp. 49–63.

Mishra, D.C. and P.S. Naidu, 1974. Two dimensional power spectral analysis of aeromagnetic fields. *Geophysical Prospecting,* Vol. **22**, pp. 345–534.

Obaje, N.G., 2009. *Geology and Mineral Resources of Nigeria*. Springer-Verlag Berlin Heidelberge. 221p. DOI:10.1007/978-3-540-92685-6.

Ofoha, C.C., G. Emujakporue and A.S. Ekine, 2018. Structural Evalution of Bouguer Gravity Data Covering Parts of Southern Niger Delta, Nigeria. *Archives of Current Research International*, Vol. **13**, no. 3, pp. 1–18. DOI:10.9734/ACRI/2018/40199.

Okpoli, C.C. and M.A. Oladunjoye, 2017. Precambrian Basement Architecture and Lineaments Mapping of Ado-Ekiti Region, using Aeromagnetic Dataset. *Geosciences Research,* Vol. **2**, No. 1, pp. 27–45.

Oyeniyi, T.O., A.A. Salami and S.B. Ojo, 2016. Magnetic surveying as an aid to geological mapping: a case study from Obafemi Awolowo University campus in Ile-Ife, Southwestern Nigeria. *Ife Journal of Science,* Vol. **18**, No. 2, pp. 331–343.

Pati, J.K., S.C. Patel, K.L. Pruseth, V.P. Malviya, M. Arima, S. Raju, P. Pati and K. Prakash, 2007. Geology and geochemistry of giant quartz veins from the Bundelkhand Craton, central India and their implications. *Journal of Earth Systematic Sciences,* **116**, 497–510.

Rabeh, T., 2011. *Tectonic Model of the Sinai Peninsula Based on Geophysical Investigations Tectonics*. Faculty of Science, Lisbon University, Portugal, pp. 93–100.

Raimi, J., B.B.M. Dewu and P. Sule, 2014. An Interpretation of Structures from the Aeromagnetic Field over a Region in the Nigerian Younger Granite Province. *International Journal of Geosciences*, Vol. **5**, 313–323.

Reid, A.B., E. Jorg and S.J. Webb. 2014. Avoidable Euler Errors – the use and abuse of Euler deconvolution applied to potential fields. *Geophysical Prospecting*, **62**, 1162–1168.

Salem, A., S. Williams, S., Fairhead, J., Ravat, D. and Smith, R. 2007. Tilt-depth method: a simple depth estimation method using first-order magnetic derivatives. *The Leading Edge*, Vol. **26**, No. 12, pp. 1502–1505.

Stavrev, P. and A.B. Reid, 2007. Degrees of homogeneity of potential fields and structural indices of Euler deconvolution. *Geophysics,* Vol. **71**, pp. 1–12.

Stavrev, P. and A.B. Reid, 2010. Euler deconvolution of gravity anomalies from thick contact/fault structures with extended negative structural index. *Geophysics,* Vol. **75**, 151–158.

Solomon, A.R., 2010. Geology, geochemistry and genesis of Amethyst mineralization and association and associated rocks in Dutse Bakura Hill, Northcentral Nigeria. Unpublished MSc project submitted to Ahmadu Bello University, Zaria.

Spector, A. and F.S. Grant, 1970. Statistical models for interpreting aeromagnetic data. *Geophysics,* Vol. **35**, 293–302.

Sultan, S.A., E. Mohamed, H.M. Abou, E.I. Mahmoud, K. Ahmed, M. Enas and E. Abd, 2017. Implementation of magnetic and gravity methods to delineate the subsurface structural features of the basement complex in central Sinai area, Egypt. *NRIAG J. of Astronomy and Geophysics,* **7**, 1, 162–174. DOI:10.1016/j.nrjag.2017.12.002.

Tatiana, F.Q. and S. Angelo, 1998. Exploration of a lignite bearing in Northern Ireland, using Maurizio ground magnetic. *Geophysics,* Vol. **62**, No. 4, pp. 1143–1150.

Telford, W.M., L.P. Geldart, R.E. Sheriff and D.A. Keys, 1990. *Applied Geophysics.* 2nd eds. Cambridge University Press. 744p.

Zhang, C., M.F. Mushayandebvu, A.B. Reid, J.D. Fairhead and M.E. Odegard, 2000. Euler deconvolution of gravity tensor gradient data. *Geophysics,* Vol. **65**, 512–520.